This is a preprint, the final version is subject to change, of the American Mineralogist (MSA)
Cite as Authors (Year) Title. American Mineralogist, in press.
(DOI will not work until issue is live.) DOI: http://dx.doi.org/10.2138/am-2016-5697

Gaussian thermoluminescence in long-range disordered K-feldspar

Luis Sánchez-Muñoz[1,*], Javier García-Guinea[2], Peter D. Townsend[3],

Tjipto Juwono[4], Ana Cremades[5]

[1]Instituto de Cerámica y Vidrio (CSIC), Kelsen 5,28049 Madrid, Spain

[2]Museo Nac. Ciencias Naturales. (CSIC), José Gutierrez Abascal 2, 28006 Madrid, Spain

[3]School of Engineering, University of Sussex, Brighton, United Kingdom

[4]Center for Econophysics, Surya University, Tangerang, Banten, Indonesia

[5]Dpto. Física de Materiales, Fac. Físicas, Univ. Compl. Madrid, 28040 Madrid, Spain

ABSTRACT

The thermoluminescence behaviour of long-range ordered crystals is usually explained by the band structure model, using and first- and second-order kinetics. However, feldspars have order-disorder phenomena and twinning, and consequently these mathematical descriptions are not helpful in most cases. In this work, the thermally stimulated intrinsic blue luminescence at 440 nm from X-ray induced defects of the K-rich feldspars is used to show a progressive behaviour change along the order-disorder series. It is observed a gradual conversion of the TL signal from a very asymmetric peak with exponential rise and power law decay in microcline and orthoclase, where a τ coefficient in log-log plots decreases with twin/domain size, to a more symmetric signal in a partially disordered sanidine, up to reach a completely symmetric Gaussian peak in fully disordered sanidine. These results are compatible with the Bässler's model of disorder, which suggest that atomic disorder involves the transformation of delocalized bands first into band tails as the source of electron traps, and later in localized density of states following a Gaussian distribution.

Always consult and cite the final, published document. See http:/www.minsocam.org or GeoscienceWorld

Keywords: K-feldspars, thermoluminescence, order-disorder series, density of states

INTRODUCTION

Solids are driven away from equilibrium after ionizing irradiation with metastable electron-hole pair formation as defects at the atomic scale. Intrinsic defect complexes are formed in which charge traps are intimately linked with subtle host lattice reorganization. In oxide wide band gap insulators, like $(K>Na)AlSi_3O_8$ (K-rich feldspars), the dissipation of the absorbed energy to lattice relaxation take place by radiative electron-hole recombination. Thermally stimulated luminescence (TL) experiments are used to analyze the relaxation phenomenon as well as to inform about their band structure. The TL phenomenon is exploited commonly for dose reconstruction methodologies, supposing that the amount of released light is directly proportional to the previous received dose. The order-disorder degree of the K-feldspar structure is intimately linked with their applicability in dosimetry applications. Feldspars exhibit a wide continuum emission band that extends from ~ 325 to 650 nm with maximum at 440 nm known as the broad blue band, found in many oxygen containing compounds. This emission in disordered feldspars is useless because of "anomalous fading", i.e. trapped electrons escape from their traps on a time scale much shorter than it is expected from the kinetics parameters determined by quantitative analysis of their TL curves. This phenomenon has been explained by "tunneling" and the increase of fading with the rise of temperature indicates that this quantum mechanical effect is thermally stimulated (Visocekas et al. 1994). J.T. Randall recognized long time ago that one of the chief problems to be solved in the mechanism of intrinsic luminescence is concerned with the extent to which the whole structure is involved, a problem that is here addressed.

Always consult and cite the final, published document. See http:/www.minsocam.org or GeoscienceWorld

Spectral analysis of the light emissions and interpretations in term of emission centres of feldspar crystals are available in literature (e.g. Krbetschek et al. 1997), but the particular effect of order-disorder states has not been addressed in detail. The samples studied in this work has been already analyzed from the spectral point of view by García-Guinea et al. (1997), Clarke et al. (1997), Clarke and Rendell (1997), and Sánchez-Muñoz et al., (2006a,b). Here, we concentrate in the 440 nm emission band only, which is observed in most K-feldspars by the majority of the luminescence techniques. The particular aim of this work is to follow the manner in which the order-disorder and the twin structures of K-rich feldspars affects the nature of the electronic structure inferred from TL data. Previous results have found a power law decays in the high temperature slope of the 290 and 440 nm emission bands in TL experiments of K-feldspars having intermediate degrees of local order, suggesting that it is an effect of disorder from long-range elastic strain fields derived from twin wall boundaries (Sánchez-Muñoz et al., 2006a, 2007a,b). This phenomenon is analyzed in detail along the order-disorder series, from the totally ordered "low microcline" end-member to the fully disordered "high sanidine" end-member (see Sánchez-Muñoz et al., 2013 for a detailed NMR characterization). In particular, we explain the highly symmetric TL signal of "high sanidine" where twin-domains are absent, as a consequence of pseudoperiodicity from atomic disorder.

EXPERIMENTAL PROCEDURE

Samples

Five K-rich feldspars have been selected for this work. Specimen *Zarz* is a perthitic K-rich feldspars Carlsbad twinned crystal of 3x2x1 cm^3 in size from a granite porphyritic rock along a fracture in Zarzalejo (Madrid, Spain), with "low microcline" X-ray diffraction

Always consult and cite the final, published document. See http:/www.minsocam.org or GeoscienceWorld

(XRD) powder pattern. Specimen *GcInt* is a blocky perthitic crystal from the intermediate zone of the Golconda III pegmatite, in Marilac district at W of Governador Valadares, Minas Gerais (Brazil), with "low microcline" XRD powder pattern. The chemical composition (by electron probe chemical analyses EPMA), luminescence emission and twin microstructures are extremely heterogeneous but intimately correlated (Sánchez-Muñoz et al. 2006b and Sánchez-Muñoz et al. 2012). Specimen *En* is a perthitic K-rich from the external zone of the Proberil pegmatite, Conselheiro Pena, Minas Gerais (Brazil), with "orthoclase" XRD powder pattern. Under the optical microscope, it shows irregular extinction close to parallel in (001) plane. A modulated structure with the typical "tweed" contrast was observed in electron microscopy, and diffuse streaks appear in electron diffraction patterns along the [001] zone axis as well as a slight deviation from 90º the γ* angle in selected area electron diffraction patterns. Some microcline unit appears close to albite veins (see Sánchez-Muñoz et al. 2012 for details). A similar specimen was studied by Sánchez-Muñoz et al. (2007a) in K-rich feldspar from Fermin pegmatite, Minas Gerais (Brazil). Specimen *Gott* is an adularia crystal from Saint Gotthard (Switzerland) with "low sanidine" X-ray diffraction pattern from St. Gotthard (Switzerland) with $Or_{93.5}Ab_{6.5}$ averaged chemical composition from EPMA. Specimen *EU2* is an unaltered transparent idiomorphic homogeneous crystal of 4x3x2 mm^3 in size crystal with "high sanidine" XRD powder pattern, from Miocene rhyolite ash fall tuffs from the Twin Fall Volcanic Field, Gooding, Idaho (USA), with $Or_{62.3}Ab_{37.5}An_{1.5}$ as averaged chemical composition from EPMA (see additional characterization in Sánchez-Muñoz et al. 2007c, and Sánchez-Muñoz et al. 2013). Albite from exsolution was not detected in specimens *Gott* and *EU2*.

Always consult and cite the final, published document. See http:/www.minsocam.org or GeoscienceWorld

Methods

Thermoluminescence spectra were performed on cleaved chips of 3x3x2 mm^3 (~5 mg) of this specimen mounted with silicone oil onto aluminum discs using the high sensitivity TL spectrometer of Sussex University (United Kingdom). Signals were recorded over the 200-800 nm wavelength range, with a resolution of 4 nm for 150 point spectra, in the range of 20-400 ºC at 2.5 ºC/minute. All signals were corrected for the spectral response of the system. X-ray induced defects where studied by TL after 50 Gy X-irradiation with a X-ray unit tube, Philips MG MCN 101, with a current of 5mA and a voltage of 5kV delivering a dose rate of 10 Gy per minute to the sample. Prior measurements, sample was stored for 24 hours under red light. Sample processing and measurements were also performed under red light to avoid electron-hole recombination from the semi-stable sites. Radioluminescence (RL) spectra were recorded during excitation using a Philips MG MCN 101 X-ray tube with a current of 15 mA and a voltage of 25 kV, delivering a dose rate of 10 Gy/min to the sample. Cathodoluminescence (CL) spectra were obtained using an electron beam with a current of 0.4 μA and a voltage of 10 kV at a room temperature. The CL image of Fig. 3b was obtained in a Hitachi S-2500, at 30 kV accelerating voltages. The light was focused by lens on the microscope window. Fig. 4c was recorded in a Leica scanning electron microscope using a bandpass filter of Lambda Research Optics, Inc. (code 430.0-F10-50.8) centered at 430 nm, FWMH = 10 nm, minimum transmittance of 50 %. CL spectra were recorded with a CCD camera, with a built-in spectrograph (Hamamatsu PMA-11) attached to the microscope window. For experimental details related to the optical and electron microscopy micrographs of Figure 3, see Sánchez-Muñoz et al. (2012).

Always consult and cite the final, published document. See http:/www.minsocam.org or GeoscienceWorld

RESULTS AND DISCUSSION

Figure 1a records the light emissions from the natural thermoluminescence (TL) spectrum in "as received" of specimen *ZARZ*. It records only light emission from "stable" centres, i.e. resistant to visible light illumination, that have been created by the ionizing radiation from environmental radioactivity. The observed emissions at 340, 400, ~ 530 and ~ 720 nm are associated with electron traps released at temperatures higher than 400 K. When this previously heated aliquot is X-irradiated with 50 Gy, after a dwell time of 24 hours under IR light, the induced thermally stimulated spectrum (ITSL) can be recorded as shown in Figure 1b. Two new emission bands from "unstable" centers appear in addition to those radiative recombinations already observed in the natural TL: i) the broad blue band with maximum at 440 nm with maxima at and ~ 400 K; and ii) an ultraviolet (UV) band at 290 nm and ~ 425 K. It is already known that these two emission bands can show power law decay in the high temperature slope of their TL spectra (Sánchez-Muñoz et al. 2007a,b). When light emissions are recorded during X-ray or electron irradiation in RL and CL experiments (Fig. 1c and 1d, respectively), defect formation is produced simultaneously to charge transfers processes and electronic transitions at recombination centers. Thus, the emission bands at 290 and 440 nm are recorded together with the 400, 530 and 720 nm bands in the RL and CL spectra. These experiments ensure the intrinsic character of the luminescence at 440 nm. Hence, ionizing radiation could involve the creation of extended defect complexes formed by recombination centers and trapped charges (see Townsend and Rowlands 1999, Sánchez-Muñoz et al. 2007a,b for details). Therefore, the particular features of the thermally stimulated radiative relaxation of these radiation-induced defects complexes were studied by ITSL experiments on samples representative of the order-disorder series.

Always consult and cite the final, published document. See http:/www.minsocam.org or GeoscienceWorld

Fig. 2 exhibits the ITL spectra of four K-feldspars along the order-disorder series, when irradiated with 50 Gy of X-ray after a dwell time of 24 hours under IR light. Disordered, untwinned and unexsolved crystals of specimens *EU2* and *Gott* do not show the 290 nm emission band, that is very sharp in ordered, twinned and exsolved ones like specimens *GcInt, ZARZ* and *En*. Disordered crystals have a light emission circa 720 nm absent in triclinic crystals. The 3D-shape of the broad blue band, represented as contour lines in the wavelength-temperature plane, changes gradually from the perfectly long-range ordered structure to the totally long-range disordered structure. The wavelength distribution of this intrinsic luminescence is very similar along the series, but drastic changes appear along the temperature axis because of the different electronic structures.

Quantitative treatment of the TL signal was performed by detailed analyses of monochromatic profiles at 440 nm along the temperature axis. This emission is interpreted as hole centres formed at the oxygen sites with electrons trapped in the vicinity of the sites of alkali atoms forming polyatomic complexes. The sharpness of the band or its constituents has not been increased by lowering the temperature, but an inner structure composed of molecular oxygen Herzberg bands is resolved in the TLS spectrum when solid argon is doped with oxygen (Schrimpf et al. 1996). A new molecular-like model of the medium-range order in K-feldspar is now available with K-O-Al multi-site correlations from high magnetic field multinuclear NMR spectroscopy (Sánchez-Muñoz et al. 2013), that helps to explain the formation of the defect complexes.

The broad blue band in the ordered feldspars (microcline and orthoclase) consists of a very asymmetric peak (Figs. 1b, 2a, 2b, 3b, 3d, and 3f). When single trap level and recombination via delocalized conduction band is considered, the glow curve must be the result of two distinct processes: the rate of escape (probability) for the trapped electrons and

Always consult and cite the final, published document. See http:/www.minsocam.org or GeoscienceWorld

the fraction of electrons remaining trapped, according to Randall and Wilkins's model. At the low temperature side, the initial rise of the peak is connected with the probability of escape *p* of electrons from the traps at depth *E*, and at temperature *T*, which is dependent on the Maxwell-Boltzmann distribution of thermal energies, and thus: $p = s \cdot e^{-E/kT}$ where *k* is the Boltzmann's and *s* varies slightly with temperature. In specimens *ZARZ*, *GcInt* and *En*, the exponential slope is associated with an activation energy value of $E_{act} \sim 0.9$ eV.

At the high temperature side, the slope of TL peak follows a power law as $\log I = -\tau \log T$ can give a linear fitting, where the slope τ is directly related to the size of twin domains. Specimen *GcInt* with large twin domains (normally larger than 10 μm, Fig.3a) has coefficient $\tau = -2.2 \pm 0.1$ (Fig. 3b, r = 0.981 and SD = 0.04 between 405 and 500 K, because it overlaps with another glow peak at higher temperature). Specimen *ZARZ* with fine twining (normally smaller than 10 μm, Fig. 3c) has $\tau = -4.0 \pm 0.1$ (Fig. 3d, r = 0.998 and SD = 0.02 between 440 and 565 K). In specimen *En* (orthoclase, partially ordered with a modulated structure in ill-defined nanodomains, Fig. 3e), $\tau = -5.5 \pm 0.1$ (Fig. 3f, r = 0.996 and SD = 0.02 between 434 and 673 K). Thus, when the slope of the high temperature side increases (i.e., when τ decreases to become more negative), the average size of the twin/domains decreases, as similar order-disorder state occurs at the local level in specimens *ZARZ* and *GcI*, and it can be interpreted as a result of disorder induced by long-range elastic strain fields (Sánchez-Muñoz et al. 2006a, 2007a,b). Since the power law behaviour is also known in the isothermal decay (Baril and Huntley 2003) as well as in induced bleaching on exposure to sunlight (Wintle 1997) of other triclinic crystals, a time-temperature superposition effect is inferred, signifying that time and temperature are equivalent to activate the same local mechanisms (Sánchez-Muñoz et al. 2007b). This

Always consult and cite the final, published document. See http:/www.minsocam.org or GeoscienceWorld

performance could be interpreted as a fundamental feature of complex systems, as already suggested for the relaxation behaviour of polymers (Glöckle and Nonnenmacher 1994), characterized by collective behaviour (Ngai et al. 1979, Jonscher 1992) of the radiation-induced defect in the crystal lattice.

Specimens *Gott* and *EU2* do not show a domain structure. The broad blue band in these disordered feldspars (sanidine) consists of a more symmetric peak (Figs. 2c and 2d) than the ordered feldspars. In "low sanidine" (specimen *Gott*) an exponential low temperature side gives a value of activation energy close to that of the ordered feldspars, but the high temperature side cannot be fitted with power law decay anymore. The disordered end-member of the "high sanidine" crystal (specimen *EU2*) shows a very symmetrical signal shape (despite of the overlapping with another emission at 400 nm typical of stable luminescent centres, Fig. 2d). It is important to note, that a Maxwell-Boltzmann distribution of thermal energies will be applicable only if a single trapping site exist. Hence, no Arrhenius type of temperature dependence can be resolved in the low temperature part of the profile, because there not exist structural sites with well defined energy values or varying in a very narrow range. Their TL peaks results from the occupational distribution of different energy level and not from a single electron-hole recombination process. Fig. 3 shows the TL profile in fully disordered sanidine, where a Gaussian fitting is compared with deconvolutions following first- and second-order kinetics using the Kitis equations (Kitis et al. 1998, Kitis 2001). A computer program was used to search for any value of the variables in these equations to obtain the best fitting, but the best fitting is obtained with a Gaussian curve, a result that must be interpreted.

Always consult and cite the final, published document. See http:/www.minsocam.org or GeoscienceWorld

IMPLICATIONS

Considering that recombination take place in electron-hole defect complexes where retrapping is negligible, changes in the long-range order (periodicity) must be essential in the relaxation process of the excited crystalline state, involving changes in charge stability, that can be interpreted as changes in the structure of bands. In perfectly ordered crystal as conventional dosimeters, trapped charges are stable and first- and second-order kinetics with an Arrhenius rise are well known phenomena based on the band theory. However, if some long-range disorder exist, it is expected that charge states in the delocalized bands are partially transformed into traps (states with quantized energy levels and localized wave function), as a continuous distribution of available energetic values for localized electron states, as band tails (Poolton et al. 2002, Jain, M. and Ankjærgaard, C. (2011), Li and Li 2013). In our interpretation intermediate degrees of local order and lattice distortions from twin wall boundaries as elastic strain fields (Sánchez-Muñoz et al., 2006a,b, 2007a,b), and lattice distortions from inclusions of impurities (Zhao et al., 2015) could have a similar effect.

When extended long-range disorder occurs, it involves the loss of strict periodicity as in sanidine where only pseudo-periodicity exist (Sánchez-Muñoz et al., 2013). Hence, the Gaussian TL signal of "high sanidine" cannot be interpreted using the conventional band model. A distribution of the trap density (exponential or Gaussian) must be associated with the occupational distribution of the density of states (DOS). The Bässler's model suggests a Gaussian DOS function for disordered solids if weak trap coupling exist, and charge localization does involve small elastic distortions and negligible polaron effect (Bässler 1981, Bässler et al. 1982, Kadashchuck et al. 1988, Arkhipov et al. 2002). In this case, the relaxation by electron-hole recombination involves a thermally activated hopping

Always consult and cite the final, published document. See http:/www.minsocam.org or GeoscienceWorld

mechanism and tunneling, instead of recombination via conduction band. Therefore, the observed Gaussian relaxation is compatible with a Gaussian DOS distribution from uncorrelated defect complexes, where "bands" have been totally transformed into "electron traps".

ACKNOWLEDGMENTS

We thank projects MAT2013-480009-C04-1-P, MAT2013-46452-C4-2-R, and CAM S2013/MIT-2753 for partial financial support.

REREFERNCES CITED

Arkhipov, V.I., Emelianova, E.V., Kadashchuk, I., Blonsky, I., Nešpůrek, S., Weiss, D.S., Bässler, H. (2002) Polaron effects on thermally stimulated photoluminescence in disordered organic systems. Physical Review Letters, 65, 165218.

Baril, M.R. & Huntley, D.J. Infrared stimulated luminescence and phosphorescence spectra of irradiated feldspars. Journal of Physics: Condensed Matter **15** 8029-8048 (2003).

Bässler, H. (1981) Localized states and electronic transport in single component organic solids with diagonal disorder. Physics Status Solidi, 107, 9-53.

Bässler, H., Schönherr, Abkowitz, M., and Pai, D.M. (1982) Hopping transport in prototypical organic glasses. Physical Review B, 26, 3105-3113.

Clarke, M.L., Rendell, H.M., Sánchez-Muñoz, L., and García-Guinea, J. (1997) A comparison of luminescence spectra and structural composition of perthitic feldspars. Radiation Measurements, 27, 137-144.

Clarke, M.L. and Rendell, H.M. (1997) Infra-red stimulated luminescence spectra of alkali feldspars. Radiation Measurements, 27, 221-236.

Always consult and cite the final, published document. See http:/www.minsocam.org or GeoscienceWorld

García-Guinea, J., Rendell, H., and Sánchez-Muñoz, L. (1997) Luminescence spectra of alkali feldspars: some relationships between structural features and luminescence emission. Radiation Protection Dosimetry, 66, 395-398.

Glöckle, W.G., Nonnenmacher, T.F. Fractional relaxation and the time-temperature superposition principle. *Rheologica Acta* **33**, 337-343 (1994).

Jain, M. and Ankjærgaard, C. (2011) Towards a non-fading signal in feldspar: Insight into charge transport and tunnelling from time-resolved optically stimulated luminescence. Radiation Measurement, 46, 292-309.

Kadashchuk, A., Ostapenko, N., Zaika, V., and Nešpůrek, S. (1998) Low-temperature thermoluminescence in poly(methyl-phenylsilylene. Chemical Physics, 234, 285-296.

Kitis, G., Gomez-Ros, J.M., and Tuyn, J.W.N. (1998) Thermoluminescence glow-curve deconvolution functions for first, second and general orders of kinetics. Journal of Physics D: Applied Physics, 31, 2636-2641.

Kitis, G. (2001) TL glow-curve deconvolution functions for various kinetic orders and continuous trap distribution: Acceptance criteria for E and s values. Journal of Radioanalytical Nuclear Chemistry, 247, 697-703.

Krbetschek, M.R., Götze, J., Dietrich, A., and Trautmann, T. (1997) Spectral information from minerals relevant for luminescence dating. Radiation Measurement, 27, 695-748.

Li, B. and Li, S.-H. (2013) The effectofband-tailstatesonthethermalstabilityoftheinfrared stimulatedluminescencefromK-feldspar. Journal of Luminescence, 136, 5–10.

Poolton, N.R.J., Ozanyan, K.B., Wallinga, W., Murray, A.S., and Bøtter-Jensen, L. (2002) Electrons in feldspar II: a consideration of the influence of conduction band-tail states on luminescence processes. Physics and Chemistry of Minerals, 29, 217-225.

Always consult and cite the final, published document. See http:/www.minsocam.org or GeoscienceWorld

Ngai, K.L, Jonscher, A.K., White, C.T. Origin of the universal dielectric response in condensed matter. Nature, 277, 185 (1979).

Sánchez-Muñoz, L., García-Guinea, J., Sanz, J., Correcher, V. and Delgado, A. (2006a) Ultraviolet luminescence from defect complexes in the twin boundaries of K-feldspar. Chemistry of Materials, 18, 3336-3342.

Sánchez-Muñoz, L., Correcher, V., Turrero, M.J., Cremades, A. and García-Guinea, J. (2006b) Visualization of elastic strain fields by the spatial distribution of the blue luminescence in a twinned microcline crystal. Physics and Chemistry of Minerals, 33, 639-650.

Sánchez-Muñoz, L., García-Guinea, J., Correcher, V. and Delgado, A. (2007a) Thermally stimulated power law relaxation of radiation-induced defects in K-feldspar. Journal of Physics: Condensed Matter, 19, 046202.

Sánchez-Muñoz, L., García-Guinea, J., Correcher, V., Delgado, A. (2007b) Radiation-induced self-structuring of radiative defects complexes in a K-feldspar crystal: A study by thermoluminescence. Radiation Measurement, 42, 775-779.

Sánchez-Muñoz, L., Correcher, V., García-Guinea, J. and Delgado, A. (2007c) Luminescence at 400 and 440 nm in sanidine feldspar from original and X-ray-induced defects. Nuclear Instruments and Methods in Physics Research A, 580, 679-682.

Sánchez-Muñoz, L., García-Guinea, J., Zagorsky, V.Ye., Juwono, T., Modreski, P.J., Cremades, A., Van Tendeloo, G., De Moura, O.J.M. (2012) The evolution of twin patterns in perthitic K-feldspar from granitic pegmatites. The Canadian Mineralogist, 50, 989-1024.

Sánchez-Muñoz, L., Sanz, J., Sobrados, I., Gan, Z.-H. (2013) Medium-range order in disordered K-feldspars by multinuclear NMR. American Mineralogist, 98, 2112-2131.

Always consult and cite the final, published document. See http:/www.minsocam.org or GeoscienceWorld

Schrimpf, A., Boekstiegel, C., Stöckmann, H.-J., Bornemanny, T., Ibbeken, K., Kraft, J. and Herkert, B. (1996) Thermally stimulated luminescence and conductivity of doped Ar solids. Journal of Physics: Condensed Matter 8, 3677-3689.

Townsend, P.D. and Rowlands, A.P. (1999) Extended defect models for thermoluminescence. Radiation Protection Dosimetry, 84, 7–12.

Visocekas, R., Spooner, N.A., Zink, A. and Blanc, P. (1994) Tunnel, afterglow, fading and infrared emission in thermoluminescence of feldspars. Radiation Measurement, 23, 377-385.

Wintle, A.G. Luminescence dating: Laboratory procedures and protocols. Radiation Measurements, 27, 769-817 (1997).

Zhao, Y., Zhou, Y., Jiang, Y., Zhou, W., Finch, A.A., Townsend, P.D., and Wang, Y. (2015) Ion size effects on thermoluminescence of terbium and europium doped magnesium orthosilicate. Journal of Material Research, 30, 3443-3452.

Figure captions

FIGURE 1. Luminescence of specimen *ZARZ* (low microcline). a) Natural TL spectrum using a contour plot, displaying wavelength λ in nm vs temperature T in K, intensity in arbitrary units (a.u.) as formlines, showing the position of luminescence bands at 340, 400, 530 and 720 nm. b) ITSL spectrum of the same aliquot after 50 Gy of X-ray, where two new emissions at 290 and 440 nm occur. c) RL spectra between 200 and 800 nm with intensity in arbitrary units (a.u.), calculated spectrum (solid line) with Gaussian curves (dashed lines) at 297, 349, 401, 439 (in blue), 530 and 714 nm, FWHM values 42, 57, 40, 74, 138 and 144 nm, respectively, r = 0.998. d) Idem CL spectrum with positions at 291,

Always consult and cite the final, published document. See http:/www.minsocam.org or GeoscienceWorld

339, 407, 450 (in blue), 526 and 712 nm, with FWHM values 52, 30, 64, 84, 123, 198 nm respectively, r = 0.999. All the analysed parameters were refined to a confidence limit of 95% accuracy.

FIGURE 2. ITSL spectra after 50 Gy X-ray in specimen *GcInt* in a) with a LM low microcline XRD powder pattern; Specimen *En* in b) with a OR orthoclase XRD powder pattern; Specimen *Gott* in c) with LS low sanidine powder pattern; and Specimen *EU2* in d) with HS high sanidine powder pattern.

FIGURE 3. Microstructures and ITSL spectra at 440 nm for specimen *GcInt*, in a) and b); specimen *ZARZ*, in c) and d); and specimen En in e) and f). a) Coarse twins > 10 μm and c) fine twins < 10 μm were obtained by transmitted light and crosses polarizers, whereas in e) the tweed pattern was resolved by transmission electron microscopy.

FIGURE 4. Minimization fitting of the luminescence emission at 440 nm in specimen *EU2* with three models. Circles are experimental point, Gaussian fit as solid line, and first-order and second-order kinetics as dotted lines (the fitting adjustment is expressed as χ^2/ν values).

Always consult and cite the final, published document. See http:/www.minsocam.org or GeoscienceWorld

This is a preprint, the final version is subject to change, of the American Mineralogist (MSA)
Cite as Authors (Year) Title. American Mineralogist, in press.
(DOI will not work until issue is live.) DOI: http://dx.doi.org/10.2138/am-2016-5697

Figure 1

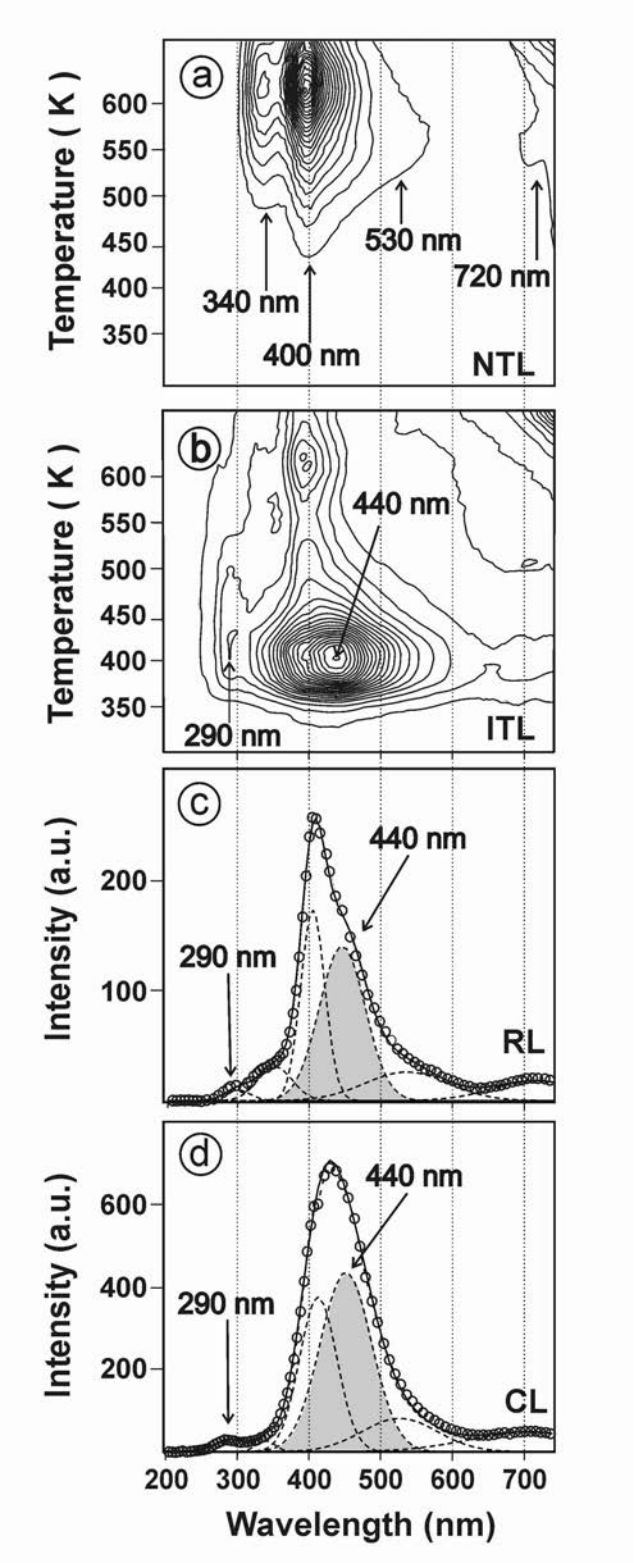

Always consult and cite the final, published document. See http:/www.minsocam.org or GeoscienceWorld

This is a preprint, the final version is subject to change, of the American Mineralogist (MSA)
Cite as Authors (Year) Title. American Mineralogist, in press.
(DOI will not work until issue is live.) DOI: http://dx.doi.org/10.2138/am-2016-5697

Figure 2

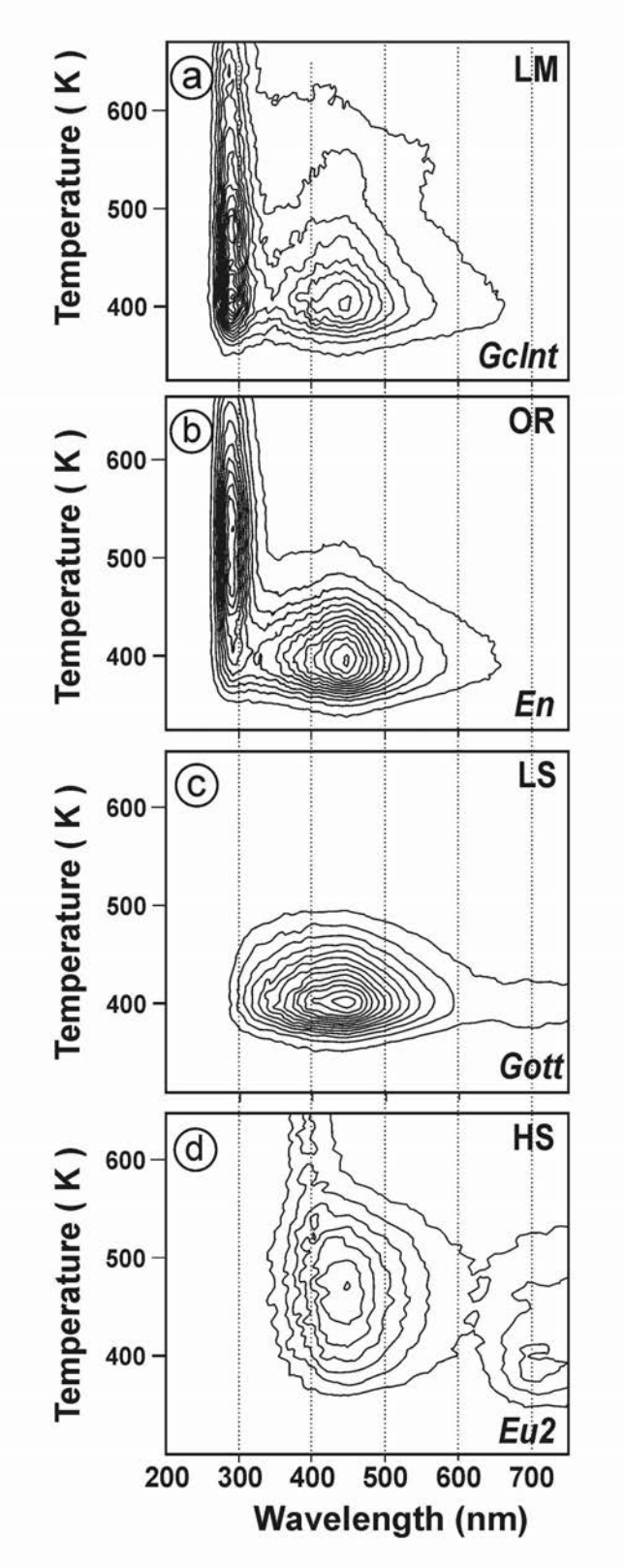

Always consult and cite the final, published document. See http:/www.minsocam.org or GeoscienceWorld

This is a preprint, the final version is subject to change, of the American Mineralogist (MSA)
Cite as Authors (Year) Title. American Mineralogist, in press.
(DOI will not work until issue is live.) DOI: http://dx.doi.org/10.2138/am-2016-5697

Figure 3

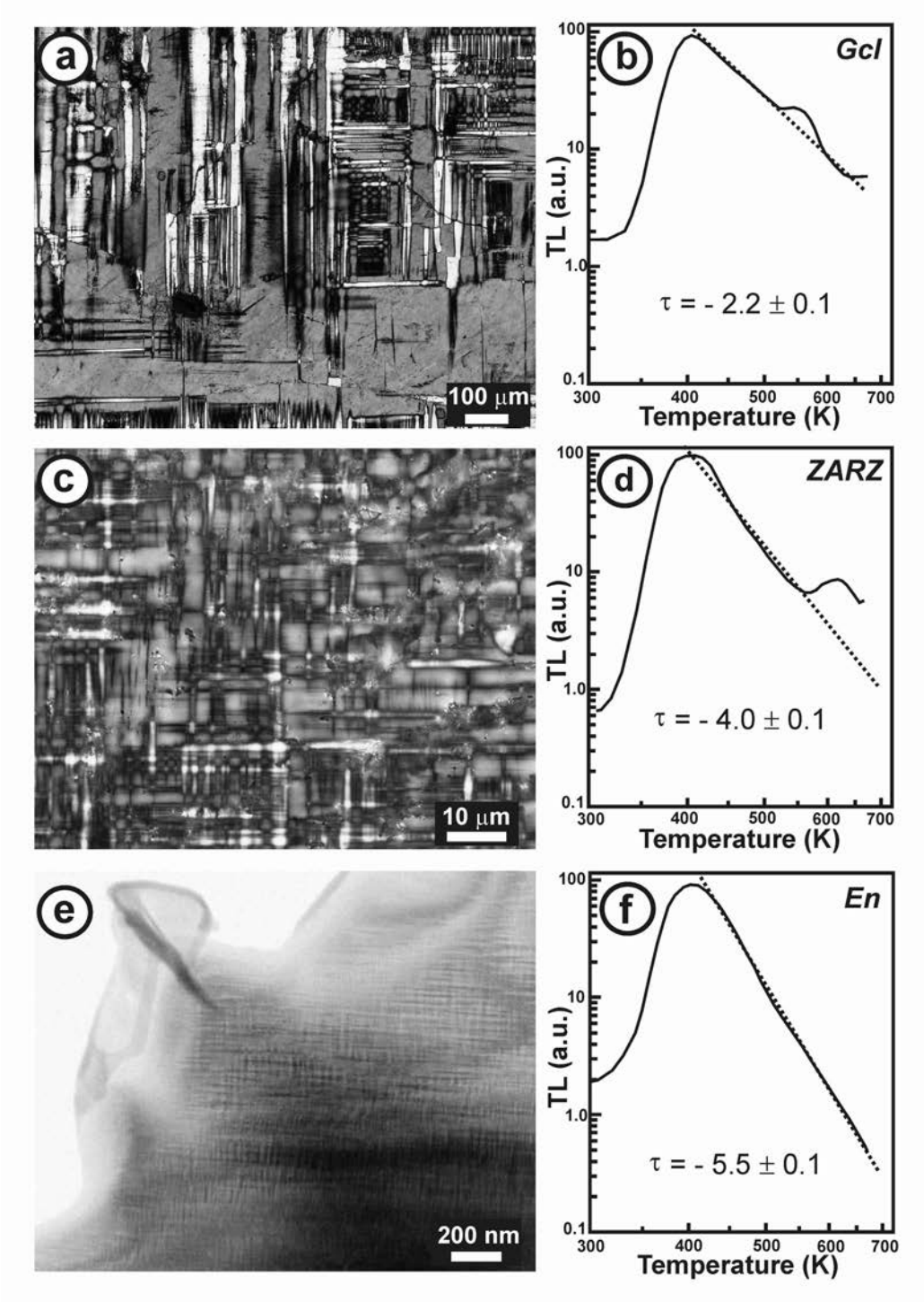

Always consult and cite the final, published document. See http:/www.minsocam.org or GeoscienceWorld

This is a preprint, the final version is subject to change, of the American Mineralogist (MSA)
Cite as Authors (Year) Title. American Mineralogist, in press.
(DOI will not work until issue is live.) DOI: http://dx.doi.org/10.2138/am-2016-5697

Figure 4

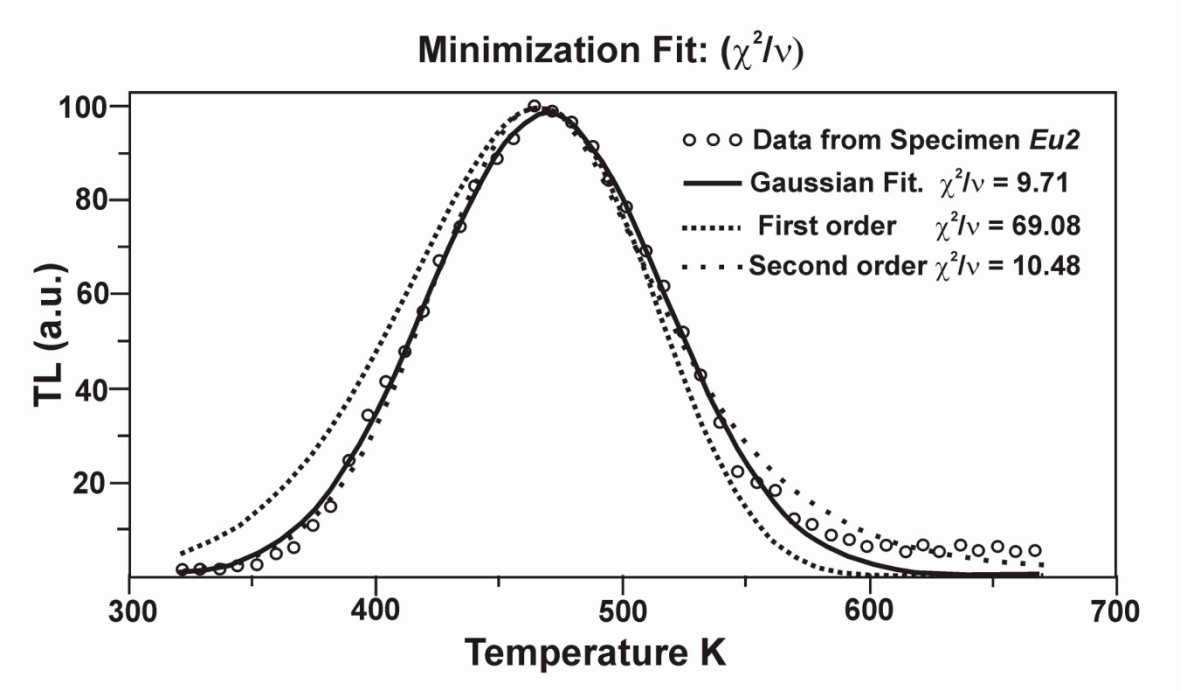

Always consult and cite the final, published document. See http:/www.minsocam.org or GeoscienceWorld